ISSN 0021-8944, Journal of Applied Mechanics and Technical Physics, 2017, Vol. 58, No. 4, pp. 670–678. © Pleiades Publishing, Ltd., 2017.
Original Russian Text © M.S. Uddin, A. Zaib, K. Bhattacharyya.

EFFECT OF THERMAL RADIATION ON HEAT TRANSFER IN AN UNSTEADY COPPER–WATER NANOFLUID FLOW OVER AN EXPONENTIALLY SHRINKING POROUS SHEET

M. S. Uddin[a], A. Zaib[b], and K. Bhattacharyya[c,d]

UDC 632.5

Abstract: The effect of thermal radiation on an unsteady boundary layer flow and heat transfer in a copper–water nanofluid over an exponentially shrinking porous sheet is investigated. With the use of suitable transformations, the governing equations are transformed into ordinary differential equations. Dual non-similarity solutions are obtained for certain values of some parameters. Owing to the presence of thermal radiation, the heat transfer rate is greatly enhanced, and the thermal boundary layer thickness decreases.

Keywords: thermal radiation, unsteady flow, heat transfer, dual non-similarity solutions, nanofluid, exponentially shrinking sheet.

DOI: 10.1134/S0021894417040113

INTRODUCTION

Investigations of nanofluids have received a lot of attention due to their vast applications in industries and engineering processes. Examples of such applications are cooling of electronic equipment, transportation, grain storage installation, chemical catalytic reactors, etc. Diffusion of medicines in blood veins also refers to nanofluid flows.

The concept of a nanofluid was first introduced by Choi and Eastman [1]. A nanofluid is a fluid containing a suspension of nanometer-sized particles of oxides, metals, carbides, nitrides, or nanotubes in a regular base fluid such as engine oil, water, ethylene glycol, etc. Most of the regular heat transfer fluids, such as grease, water, oil, etc., have poor thermal conductivities, which are insufficient to meet the necessity of today's requirement of a rapid rate of cooling. A reliable method to improve the thermal conductivity is to add nanoparticles into the base fluid. Nanofluids are also important for the production of nanostructured materials [2], for the engineering of complex fluids [3], as well as for cleaning oil from surfaces [4] due to their excellent wetting and spreading behavior. The heat transfer in a boundary layer flow past a stretching/shrinking sheet has many applications in real world problems: paper production, glass fiber production, hot rolling, etc.

Crane [5] was the first researcher who studied a boundary layer flow on a linearly stretching sheet. The heat transfer analysis of this problem was discussed by Gupta and Gupta [6]. The flow over a shrinking sheet was investigated by Wang [7]. Miklavčič and Wang [8] obtained the conditions of existence and uniqueness of the similarity solution of the shrinking sheet problem. A boundary layer flow and heat transfer developed due to stretching of a

[a]Mathematics Discipline, Khulna University, Khulna-9208, Bangladesh; sharif_ku@yahoo.com. [b]Department of Mathematical Sciences, Federal Urdu University of Arts, Science and Technology, Gulshan-e-Iqbal Karachi, Pakistan; zaib20042002@yahoo.com. [c]Department of Mathematics, Institute of Science, Banaras Hindu University, Varanasi-221005, Uttar Pradesh, India; krish.math@yahoo.com. [d]Department of Mathematics, The University of Burdwan, Burdwan-713104, West Bengal, India (previous affiliation); krish.math@yahoo.com. Translated from Prikladnaya Mekhanika i Tekhnicheskaya Fizika, Vol. 58, No. 4, pp. 115–125, July–August, 2017. Original article submitted November 6, 2014; revision submitted May 17, 2016.

sheet with an exponentially varying velocity were analyzed by Magyari and Keller [9]. Bhattacharyya [10] investigated a steady flow and heat transfer over an exponentially shrinking sheet subjected to suction. The first report on a nanofluid flow in the boundary layer case due to a linearly stretching sheet was published by Khan and Pop [11]. Nadeem and Lee [12] derived analytical solutions by using the homotopy analysis method for a nanofluid flow past an exponentially stretching sheet. Bachok et al. [13] investigated a boundary layer flow near the stagnation point in a nanofluid toward a stretching/shrinking sheet. Hamad and Ferdows [14] obtained a similarity solution for the flow and heat transfer over a nonlinearly stretching sheet in a nanofluid. Bachok et al. [15] studied a stagnation-point flow and heat transfer in a copper–water nanofluid over a stretching/shrinking sheet. A mixed convection flow of a copper–water nanofluid near a stagnation point toward a shrinking sheet was investigated by Das [16]. Makinde et al. [17] studied a combined effect of the MHD buoyancy force and heat transfer near a stagnation point of a nanofluid flow over a stretching/shrinking sheet. Haile and Shankar [18] investigated a boundary layer flow and heat transfer of a nanofluid over a moving permeable flat surface. A steady boundary layer flow and heat transfer of a nanofluid due to a nonlinearly stretching/shrinking porous sheet were studied by Zaimi et al. [19].

Time-dependent shrinking sheet flows yield some new important results of flow dynamics. An unsteady boundary layer flow over a shrinking sheet with suction was examined by Fang et al. [20], and an unsteady boundary-layer flow of an electrically conducting fluid over a flat shrinking sheet was investigated by Merkin and Kumaran [21]. Yacob et al. [22] studied a two-dimensional unsteady boundary layer flow of a non-Newtonian power-law fluid on a shrinking sheet. An unsteady boundary layer and heat transfer near the stagnation point toward a shrinking/ stretching sheet were considered by Bhattacharyya [23].

Bachok et al. [24] reported an unsteady boundary layer flow of a nanofluid over a permeable linearly stretching/shrinking sheet.

The inclusion of the thermal radiation effect on heat transfer in a boundary layer flow makes the problem more realistic and interesting. In the literature, there are very few articles on the effects of thermal radiation on an unsteady boundary layer flow induced by a shrinking sheet. Viskanta and Grosh [25] discussed a boundary layer flow and heat transfer over a wedge, taking into consideration the effect of thermal radiation. Pal [26] studied the effect of the buoyancy force on heat and mass transfer in a stagnation-point flow over a stretching sheet in the presence of thermal radiation. Bhattacharyya et al. [27] showed the effects of thermal radiation on a stagnation-point flow and heat transfer over a permeable shrinking sheet. Mukhopadhyay et al. [28] obtained a similarity solution for a boundary layer flow and heat transfer over a moving plate with the thermal radiation effect. Bhattacharyya et al. [29] demonstrated the radiation effects on a micropolar fluid flow and heat transfer due to a porous shrinking sheet. Mukhopadhyay and Gorla [30] investigated the effect of thermal radiation on a boundary layer flow and heat transfer over a porous exponentially stretching sheet. Nadeem and Haq [31] studied the radiation effect on an MHD flow of a nanofluid over a stretching sheet under a convective boundary condition.

The problem of an unsteady nanofluid flow over an exponentially shrinking sheet in the presence of thermal radiation is investigated in the present study.

1. MATHEMATICAL FORMULATION

Let us consider an unsteady flow of an incompressible nanofluid on an exponentially shrinking porous flat sheet in the presence of thermal radiation. The base fluid is water, which contains copper nanoparticles. The governing boundary layer equations of motion and the energy equation have the following form [24, 32]:

$$\frac{\partial u}{\partial x} + \frac{\partial v}{\partial y} = 0; \tag{1}$$

$$\frac{\partial u}{\partial t} + u\,\frac{\partial u}{\partial x} + v\,\frac{\partial u}{\partial y} = \frac{\mu_{nf}}{\rho_{nf}}\,\frac{\partial^2 u}{\partial y^2}; \tag{2}$$

$$\frac{\partial T}{\partial t} + u\,\frac{\partial T}{\partial x} + v\,\frac{\partial T}{\partial y} = \alpha_{nf}\,\frac{\partial^2 T}{\partial y^2} - \frac{1}{(\rho c_p)_{nf}}\,\frac{\partial q_r}{\partial y}. \tag{3}$$

System (1)–(3) is subjected to the initial and boundary conditions

$$\begin{aligned} &t<0: \qquad u=0, \quad v=0, \quad T=T_\infty, \\ &t\geqslant 0: \qquad u=-U_w, \quad v=-v_w, \quad T=T_w(x,t)=T_\infty+T_0\,\mathrm{e}^{x/(2L)}/(1-\gamma t), \quad y=0, \\ &\qquad\quad u\to 0, \quad T\to T_\infty, \quad y\to\infty. \end{aligned} \tag{4}$$

In Eqs. (1)–(4), u and v are the velocity components in the x and y directions, respectively, $U_w=a\,\mathrm{e}^{x/L}/(1-\gamma t)$ is the variable shrinking velocity of the sheet with $a>0$ and $\gamma>0$ being constants having dimensions [m/s] and [s^{-1}], respectively, and L being the reference length, $v_w=v_0\,\mathrm{e}^{x/(2L)}/\sqrt{1-\gamma t}$ is the variable suction velocity with $v_0>0$ being a constant, T is the temperature, q_r is the radiative flux, T_w is the variable wall temperature, T_0 is the reference temperature, T_∞ is the constant temperature in the free stream, μ_{nf} is the viscosity of the nanofluid, ρ_{nf} is the density of the nanofluid, α_{nf} is the thermal diffusivity of the nanofluid, and $(\rho c_p)_{nf}$ is the specific heat parameter of the nanofluid defined as follows [33]:

$$\mu_{nf}=\frac{\mu_f}{(1-\varphi)^{2.5}}, \qquad \rho_{nf}=(1-\varphi)\rho_f+\varphi\rho_s, \qquad \alpha_{nf}=\frac{k_{nf}}{(\rho c_p)_{nf}},$$

$$(\rho c_p)_{nf}=(1-\varphi)(\rho c_p)_f+\varphi(\rho c_p)_s, \qquad \frac{k_{nf}}{k_f}=\frac{k_s+2k_f-2\varphi(k_f-k_s)}{k_s+2k_f+\varphi(k_f-k_s)}.$$

Here φ is the solid volume fraction of the nanofluid, k_{nf} is the thermal conductivity of the nanofluid, μ_f is the viscosity of the base fluid, k_f is the thermal conductivity of the base fluid, k_s is the thermal conductivity of the solid particles, $(\rho c_p)_f$ is the specific heat parameter of the base fluid, and $(\rho c_p)_s$ is the specific heat parameter of the solid particles. Using Rosseland's approximation for radiation [34], we have

$$q_r=-\frac{4\sigma^*}{3k^*}\,\frac{\partial T^4}{\partial y}$$

(σ^* is the Stefan–Boltzmann constant and k^* is the absorption coefficient). We presume that the temperature variation within the flow is such that T^4 may be expanded in a Taylor series. Expanding T^4 about T_∞ and neglecting higher-order terms, we obtain

$$T^4\simeq 4T_\infty^3T-3T_\infty^4. \tag{5}$$

In view of Eq. (5), Eq. (3) reduces to

$$\frac{\partial T}{\partial t}+u\,\frac{\partial T}{\partial x}+v\,\frac{\partial T}{\partial y}=\alpha_{nf}\,\frac{\partial^2 T}{\partial y^2}+\frac{16\sigma^*T_\infty^3}{3k^*(\rho c_p)_{nf}}\,\frac{\partial^2 T}{\partial y^2}. \tag{6}$$

Let us introduce the following transformations:

$$\begin{aligned} &u=\frac{a}{1-\gamma t}\,\mathrm{e}^{x/L}\,f'(\eta), \qquad v=-\sqrt{\frac{av_f}{2L(1-\gamma t)}}\;\mathrm{e}^{x/(2L)}[f(\eta)+\eta f'(\eta)], \\ &\eta=\sqrt{\frac{a}{2Lv_f(1-\gamma t)}}\;\mathrm{e}^{x/(2L)}\,y, \qquad \theta(\eta)=\frac{T-T_\infty}{T_w-T_\infty}. \end{aligned} \tag{7}$$

In variables (7), Eqs. (2) and (6) transforms into the nonlinear ordinary differential equations

$$\begin{aligned} &\frac{1}{(1-\varphi)^{2.5}(1-\varphi+\varphi\,\rho_s/\rho_f)}\,f'''+ff''-2f'^2-A(2f'+\eta f'')=0, \\ &\frac{k_{nf}/k_f}{\mathrm{Pr}\,[1-\varphi+\varphi(\rho c_p)_s/(\rho c_p)_f]}\,\theta''+\frac{3N}{3N+4}\,[f\theta'-f'\theta-A(2\theta+\eta\theta')]=0, \end{aligned} \tag{8}$$

and the boundary conditions are converted to the form

$$f(0)=S, \quad f'(0)=-1, \quad \theta(0)=1, \quad f'(\infty)\to 0, \quad \theta(\infty)\to 0, \tag{9}$$

where the prime denotes differentiation with respect to η, $\mathrm{Pr}=v_f/\alpha_f$ is the Prandtl number, $N=k_{nf}k^*/(4\sigma^*T_\infty^3)$ is the thermal radiation parameter, $S=v_0\sqrt{2L/(av_f)}>0$ is the suction parameter, and $A=\gamma L\,\mathrm{e}^{-x/L}/a$ is the

Thermophysical properties of water and copper nanoparticles

Nanofluid component	C_p, J/(kg · K)	ρ, kg/m^3	k, W/(m · K)	$\alpha \cdot 10^{-7}$, m^2/s
Water	4179	997.1	0.613	1.47
Copper particles	385	8933	400	1163.1

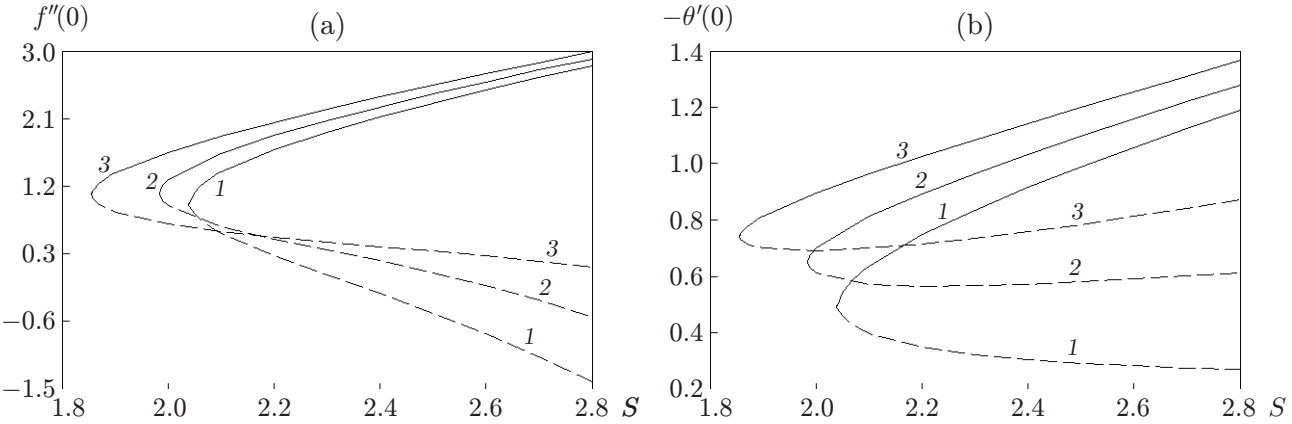

Fig. 1. Variations of $f''(0)$ (a) and $-\theta'(0)$ (b) with S for $\varphi = 0.05$, Pr $= 1$, $N = 2$, and different values of the unsteady parameter: $A = 0$ (*1*), 0.2 (*2*), and 0.4 (*3*); the solid and dashed curves show the first and second solutions, respectively.

unsteady parameter. At $A \neq 0$, the flow is unsteady, and the solution derived in this work is not a similarity solution. At $A = 0$, the flow is steady, and a similarity solution can be obtained.

The physical quantities of interest are the local skin friction coefficient and the local Nusselt number, which are defined as

$$C_f = \frac{\mu_{nf}}{\rho_f U_w^2}\Big(\frac{\partial u}{\partial y}\Big)\Big|_{y=0}, \qquad \mathrm{Nu}_x = -\frac{x k_{nf}}{k_f (T_w - T_\infty)}\Big(\Big(1 + \frac{16\sigma^* T_\infty^3}{3 k_{nf} k^*}\Big)\frac{\partial T}{\partial y}\Big)\Big|_{y=0},$$

or

$$C_f \,\mathrm{Re}_x^{1/2}\sqrt{\frac{2L}{x}} = \frac{1}{(1-\varphi)^{2.5}}\, f''(0), \qquad \mathrm{Nu}_x \,\mathrm{Re}_x^{-1/2}\sqrt{\frac{2L}{x}} = -\frac{k_{nf}}{k_f}\,\frac{3N+4}{3N}\,\theta'(0),$$

where $\mathrm{Re}_x = x U_w / v_f$ is the local Reynolds number.

2. RESULTS AND DISCUSSION

The system of transformed nonlinear ordinary differential equations (8) under the boundary conditions (9) was solved numerically by using the Matlab package for various values of the involved physical parameters, i.e., unsteady parameter A, radiation parameter N, nanoparticle volume fraction φ, Prandtl number Pr , and suction parameter S. The thermophysical properties of the considered base fluid (water) and copper nanoparticles are listed in the table.

The skin friction coefficient $f''(0)$ and the heat transfer coefficient $-\theta'(0)$ are plotted in Fig. 1 as functions of the suction parameter S for different values of the unsteady parameter A. The results show that the values of $f''(0)$ and $-\theta'(0)$ increase with increasing A. In the steady case ($A = 0$), dual similarity solutions are observed for $S \geqslant 2.038$ and no solutions are obtained for the flow with $S < 2.038$. In the unsteady case with $A = 0.2$, there are two non-similarity solutions for $S \geqslant 1.985$, and no solutions are found for $S < 1.985$. For $A = 0.4$, there are two non-similarity solutions for $S \geqslant 1.856$, and no solutions exist for $S < 1.856$. Thus, it is interesting to note that the lower boundary of the interval of the suction parameter S in which two solutions exist decreases with increasing unsteady parameter A.

The graphs of $f''(0)$ and $-\theta'(0)$ as functions of S for different values of the nanoparticle volume fraction parameter φ are shown in Fig. 2.

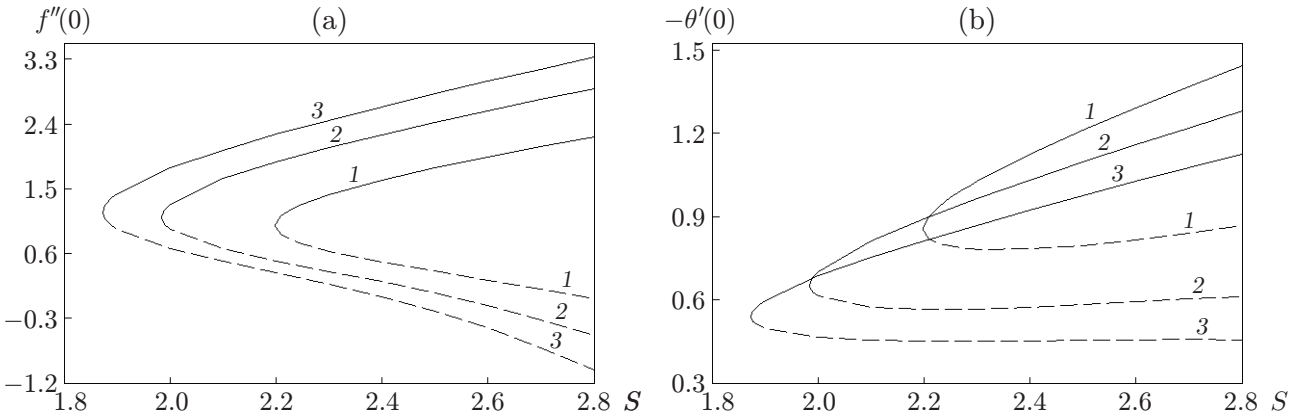

Fig. 2. Variations of $f''(0)$ (a) and $-\theta'(0)$ (b) with S for $A = 0.2$, Pr $= 1$, $N = 2$, and different values of the nanoparticle volume fraction parameter: $\varphi = 0$ (*1*), 0.05 (*2*), and 0.10 (*3*): the solid and dashed curves show the first and second solutions, respectively.

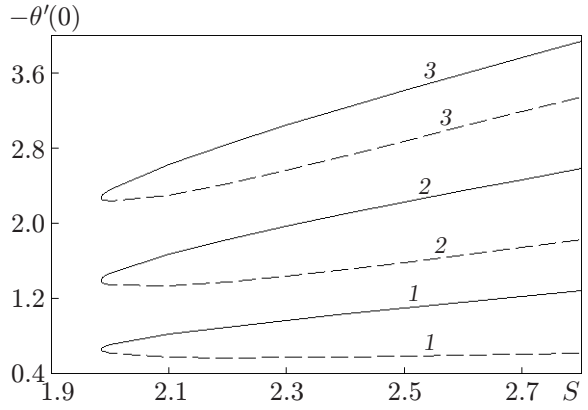

Fig. 3.

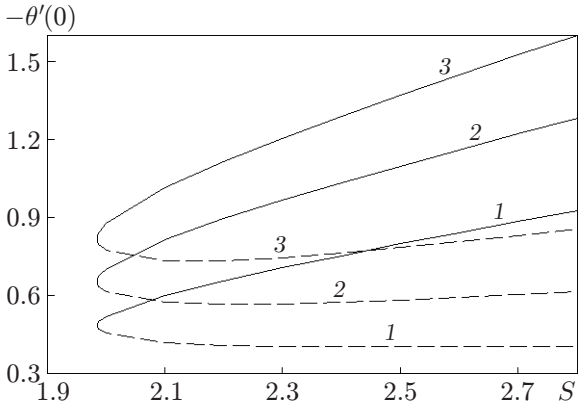

Fig. 4.

Fig. 3. Variations of $-\theta'(0)$ with S for $A = 0.2$, $\varphi = 0.05$, $N = 2$, and different values of the Prandtl number: Pr $= 1$ (*1*), 2 (*2*), and 3 (*3*); the solid and dashed curves show the first and second solutions, respectively.

Fig. 4. Variations of $-\theta'(0)$ with S for $A = 0.2$, $\varphi = 0.05$, Pr $= 1$ and different values of the radiation parameter: $N = 1$ (*1*), 2 (*2*), and 4 (*3*); the solid and dashed curves show the first and second solutions, respectively.

For the first solution, the value of $f''(0)$ increases with increasing φ; for the second solution, the value of $f''(0)$ decreases with increasing φ (see Fig. 2a). On the other hand, Fig. 2b shows that the value of $-\theta'(0)$ decreases with increasing φ for both solutions.

It is also worth mentioning that integration with respect to η has been performed until the asymptotic convergence with the far field boundary conditions with desired accuracy was reached.

For each value of φ, there is a critical value S_c of the suction parameter S such that the dual solutions exist at $S > S_c$. For $A = 0.2$, the critical values are $S_c = 2.199$, 1.985, and 1.874 for $\varphi = 0$, 0.05, and 0.10, respectively. Due to the presence of nanoparticles in the base fluid (with increasing φ), the critical value S_c decreases.

The behavior of the heat transfer coefficient $-\theta'(0)$ as a function of S for different values of the Prandtl number Pr and radiation parameter N is illustrated in Figs. 3 and 4. It is observed that the values of $-\theta'(0)$ increase with increasing Prandtl number and radiation parameter for both the first and second solutions. This means that the heat transfer rate in a moving fluid is enhanced due to the thermal radiation effect.

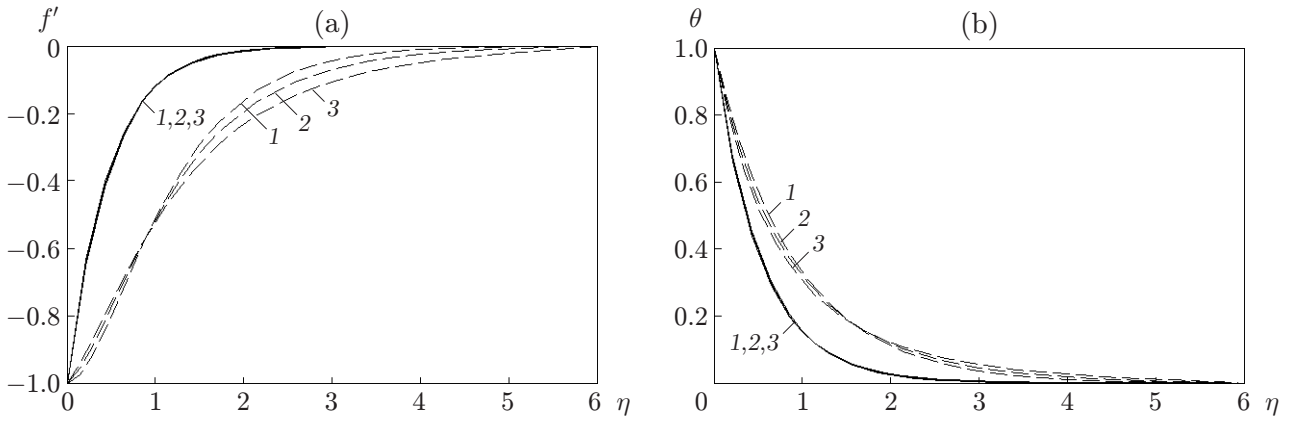

Fig. 5. Velocity (a) and temperature (b) profiles across the boundary layer for $\varphi = 0.05$, $S = 2.3$, $\mathrm{Pr} = 2$, $N = 2$, and different values of the unsteady parameter: $A = 0$ (*1*), 0.1 (*2*), and 0.2 (*3*); the solid and dashed curves show the first and second solutions, respectively.

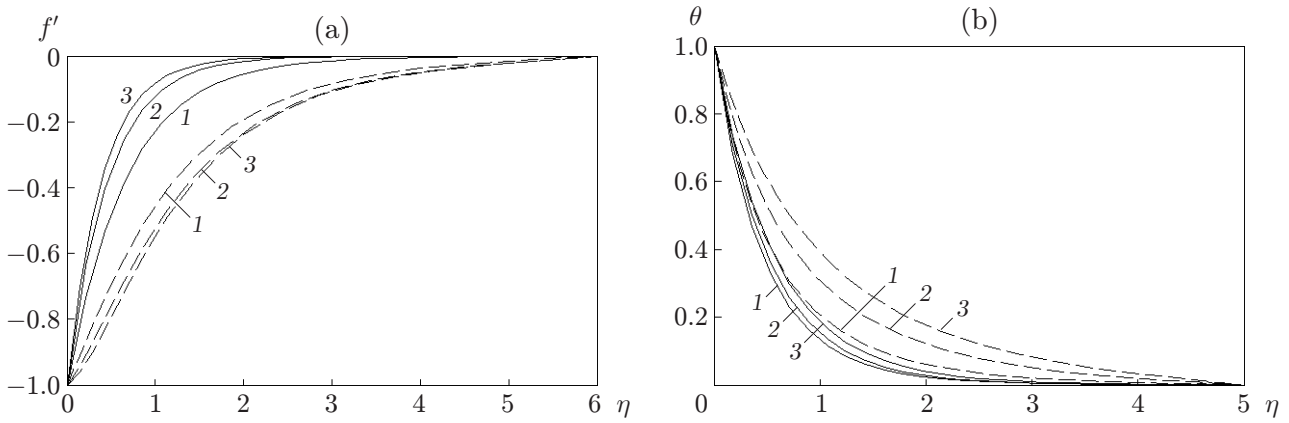

Fig. 6. Velocity (a) and temperature (b) profiles across the boundary layer for $A = 0.2$, $S = 2.3$, $\mathrm{Pr} = 2$, $N = 2$, and different values of the nanoparticle volume fraction parameter: $\varphi = 0$ (*1*), 0.05 (*2*), and 0.10 (*3*); the solid and dashed curves show the first and second solutions, respectively.

The velocity and temperature profiles across the boundary layer for various values of the unsteady parameter A are depicted in Fig. 5. It is seen that the flow velocity increases with increasing A near the sheet and decreases far away from the sheet. Thus, the velocity boundary layer thickness increases with increasing A. The thermal boundary layer also becomes thicker with increasing A. The boundary layer thickness is smaller for the first solution than for the second solution.

The effect of the nanoparticle volume fraction φ on the velocity and temperature profiles across the boundary layer is presented in Fig. 6. The fluid velocity inside the boundary layer increases with increasing φ for the first solution and decreases for the second solution. The temperature increases at all points for both solutions; consequently, the thermal boundary layer thickness increases. The increase in temperature is caused by enhancement of the thermal conductivity of the nanofluid with increasing volume fraction of nanoparticles.

Suction plays an important role to maintain the boundary layer flow near the sheet by controlling the generated vorticity due to shrinking. Figure 7 illustrates the velocity and temperature profiles across the boundary layer for different values of the suction parameter S. It is seen that the velocity increases with increasing S for the first solution and decreases for the second solution (see Fig. 7a). The thermal boundary layer thickness decreases with increasing S for both solutions (see Fig. 7b). Actually, due to suction, the fluid layers are brought closer to the surface to prevent the diffusion of vorticity.

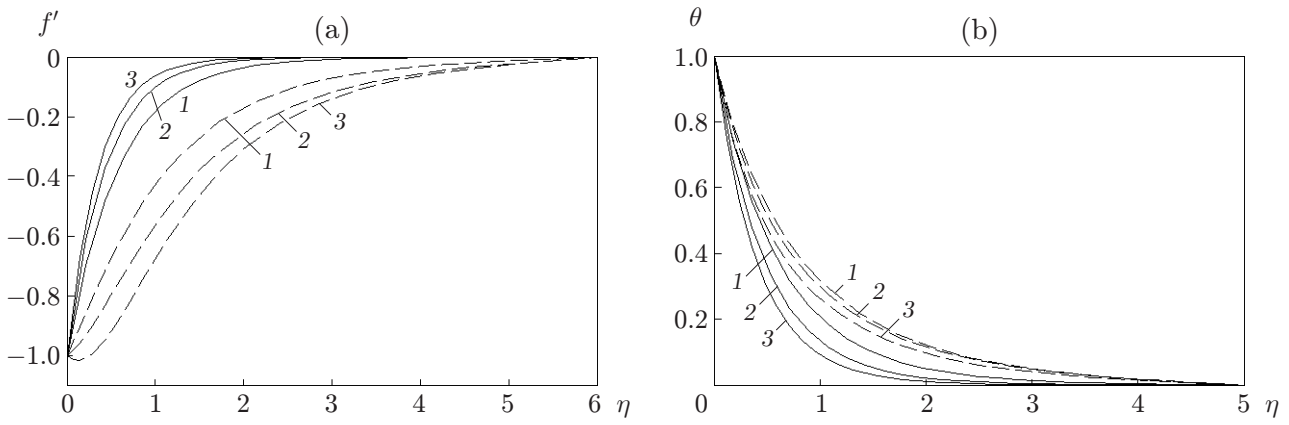

Fig. 7. Velocity (a) and temperature (b) profiles across the boundary layer for $A = 0.2$, $\varphi = 0.05$, $\mathrm{Pr} = 2$, $N = 2$, and different values of the suction parameter: $S = 2.1$ (*1*), 2.4 (*2*), and 2.7 (*3*); the solid and dashed curves show the first and second solutions, respectively.

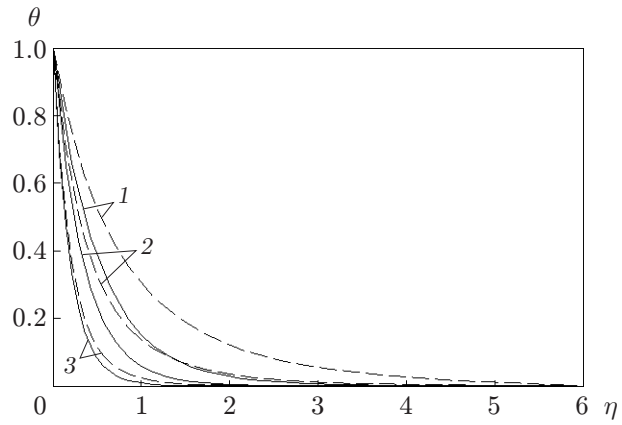

Fig. 8.

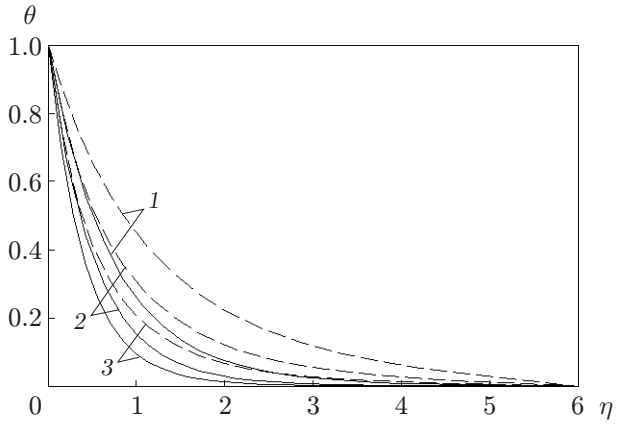

Fig. 9.

Fig. 8. Temperature profiles across the boundary layer for $A = 0.2$, $\varphi = 0.05$, $S = 2.3$, $N = 2$, and different values of the Prandtl number: $\mathrm{Pr} = 2$ (*1*), 3 (*2*), and 5 (*3*); the solid and dashed curves show the first and second solutions, respectively.

Fig. 9. Temperature profiles across the boundary layer for $A = 0.2$, $\varphi = 0.05$, $S = 2.3$, $\mathrm{Pr} = 2$, and different values of the radiation parameter: $N = 1$ (*1*), 2 (*2*), and 4 (*3*); the solid and dashed curves show the first and second solutions, respectively.

Figures 8 and 9 show the temperature profiles across the boundary layer for different values of the Prandtl number and radiation parameter, respectively. The fluid temperature decreases with increasing Prandtl number for both solutions (see Fig. 8). Similarly, the fluid temperature and the thermal boundary layer thickness decrease with increasing radiation parameter N for both solutions (see Fig. 9).

CONCLUSIONS

The problem of an unsteady boundary layer flow and heat transfer of a copper–water nanofluid over a permeable exponentially shrinking sheet with thermal radiation effects is solved numerically. The original problem is reduced to a boundary-value problem for two ordinary differential equations. Dual non-similarity solutions of

the problem are obtained for different values of the governing physical parameters. From this study, the following conclusions can be drawn.

The skin friction coefficient and the heat transfer coefficient increase with increasing unsteady parameter.

The heat transfer coefficient increases in the presence of thermal radiation with increasing Prandtl number. The fluid temperature inside the boundary layer decreases with increasing radiation parameter.

The skin friction coefficient and fluid velocity increase with increasing nanoparticle volume fraction parameter for both solutions, while the heat transfer coefficient decreases.

An increase in the nanoparticle volume fraction leads to expansion of the range of the suction parameter in which non-similar solutions exist.

One of the authors, K. Bhattacharyya is grateful to the National Board for Higher Mathematics (NBHM), Department of Atomic Energy, Government of India for the financial support in pursuing this work.

REFERENCES

1. S. U. S. Choi and J. A. Eastman, "Enhancing Thermal Conductivity of Fluids with Nanoparticles," in *Proc. of the ASME Int. Mech. Eng. Congress and Exposition, San Francisco, November 12–17, 1995* (ASME, New York, 1995), FED V. 231/MD V. 66, pp. 99–105.
2. I. A. Kinloch, S. A. Roberts, and A. H. Windle, "A Rheological Study of Concentrated Aqueous Nanotube Dispersions," Polymer **43**, 7483–7491 (2002).
3. V. Tohver, A. Chan, O. Sakurada, and J. A. Lewis, "Nanoparticle Engineering of Complex Fluid Behaviour," Langmuir **17**, 8414–8421 (2001).
4. D. T. Wasan and A. D. Nikolov, "Spreading of Nanofluids on Solids," Nature **423**, 156–159 (2003).
5. L. J. Crane, "Flow Past a Stretching Plate," Z. Angew. Math. Phys. **21**, 645–647 (1970).
6. P. S. Gupta and A. S. Gupta, "Heat and Mass Transfer on a Stretching Sheet with Suction and Blowing," Canad. J. Chem. Eng. **55**, 744–746 (1977).
7. C. Y. Wang, "Liquid Film on an Unsteady Stretching Sheet," Quart. Appl. Math. **48**, 601–610 (1990).
8. Miklavčič and C. Y. Wang, "Viscous Flow due a Shrinking Sheet," Quart. Appl. Math. **64**, 283–290 (2006).
9. E. Magyari and B. Keller, "Heat and Mass Transfer in the Boundary Layers on an Exponentially Stretching Continuous Surface," J. Phys., D: Appl. Phys. **32**, 577–585 (1999).
10. K. Bhattacharyya, "Boundary Layer Flow and Heat Transfer over an Exponentially Shrinking Sheet," Chinese Phys. Lett. **28**, 074701 (2011).
11. W. A. Khan and I. Pop, "Boundary-Layer Flow of a Nanofluid Past a Stretching Sheet," Int. J. Heat Mass Transfer **53**, 2477–2483 (2010).
12. S. Nadeem and C. Lee, "Boundary Layer Flow of Nanofluid Over an Exponentially Stretching Surface," Nanoscale Res. Lett. **7**, 94 (2012).
13. N. Bachok, A. Ishak, and I. Pop, "Stagnation-Point Flow Over a Stretching/Shrinking Sheet in a Nanofluid," Nanoscale Res. Lett. **6**, 623–633 (2011).
14. M. A. A. Hamad and M. Ferdows, "Similarity Solutions to Viscous Flow and Heat Transfer of Nanofluid over Nonlinearly Stretching Sheet," Appl. Math. Mech. (English Ed.) **33**, 923–930 (2012).
15. N. Bachok, A. Ishak, R. Nazar, and N. Senu, "Stagnation-Point Flow over a Permeable Stretching/Shrinking Sheet in a Copper–Water Nanofluid," Boundary Value Problems **39**, 1–10 (2013).
16. K. Das, "Mixed Convection Stagnation Point Flow and Heat Transfer of Cu–Water Nanofluids Towards a Shrinking Sheet," Heat Transfer—Asian Res. **42**, 230–242 (2013).
17. O. D. Makinde, W. A. Khan, and Z. H. Khan, "Buoyancy Effects on MHD Stagnation Point Flow and Heat Transfer of a Nanofluid Past a Convectively Heated Stretching/Shrinking Sheet," Int. J. Heat Mass Transfer **62**, 526–533 (2013).
18. E. Haile and B. Shankar, "A Steady MHD Boundary-Layer Flow of Water-Based Nanofluids over a Moving Permeable Flat Plate," Int. J. Math. Res. **4**, 27–41 (2015).
19. K. Zaimi, A. Ishak, and I. Pop, "Boundary Layer Flow and Heat Transfer over a Nonlinearly Permeable Stretching/Shrinking Sheet in a Nanofluid," Sci. Rep. **4**, 4404 (2014).
20. T. G. Fang, J. Zhang, and S. S. Yao, "Viscous Flow over an Unsteady Shrinking Sheet with Mass Transfer," Chinese Phys. Lett. **26**, 014703 (2009).

21. J. H. Merkin and V. Kumaran, "The Unsteady MHD Boundary-Layer Flow on a Shrinking Sheet," Eur. J. Mech., B: Fluids **29**, 357–363 (2010).
22. N. A. Yacob, A. Ishak, and I. Pop, "Unsteady Flow of a Power-Law Fluid Past a Shrinking Sheet with Mass Transfer," Z. Naturforsch. **67a**, 65–69 (2012).
23. K. Bhattacharyya, "Heat Transfer Analysis in Unsteady Boundary Layer Stagnation-Point Flow Towards a Shrinking/Stretching Sheet," Ain Shams Eng. J. **4**, 259–264 (2013).
24. N. Bachok, A. Ishak, and I. Pop, "Unsteady Boundary-Layer Flow and Heat Transfer of a Nanofluid over a Permeable Stretching/Shrinking Sheet," Int. J. Heat Mass Transfer **55**, 2102–2109 (2012).
25. R. Viskanta and R. J. Grosh, "Boundary Layer in Thermal Radiation Absorbing and Emitting Media," Int. J. Heat Mass Transfer **5**, 795–806 (1962).
26. D. Pal, "Heat and Mass Transfer in Stagnation-Point Flow Towards a Stretching Surface in the Presence of Buoyancy Force and Thermal Radiation," Meccanica **44**, 145–158 (2009).
27. K. Bhattacharyya, S. Mukhopadhyay, and G. C. Layek, "Slip Effects on Boundary Layer Stagnation-Point Flow and Heat Transfer Towards a Shrinking Sheet," Int. J. Heat Mass Transfer **54**, 308–313 (2011).
28. S. Mukhopadhyay, K. Bhattacharyya, and G. C. Layek, "Steady Boundary Layer Flow and Heat Transfer over a Porous Moving Plate in Presence of Thermal Radiation," Int. J. Heat Mass Transfer **54**, 2751–2757 (2011).
29. K. Bhattacharyya, S. Mukhopadhyay, G. C. Layek, and I. Pop, "Effects of Thermal Radiation on Micropolar Fluid Flow and Heat Transfer over a Porous Shrinking Sheet," Int. J. Heat Mass Transfer **55**, 2945–2952 (2012).
30. S. Mukhopadhyay and R. S. R. Gorla, "Effects of Partial Slip on Boundary Layer Flow Past a Permeable Exponential Stretching Sheet in Presence of Thermal Radiation," Heat Mass Transfer **48**, 1773–1781 (2012).
31. S. Nadeem and R. U. Haq, "Effect of Thermal Radiation for Magnetohydrodynamic Boundary Layer Flow of a Nanofluid Past a Stretching Sheet with Convective Boundary Condition," J. Comput. Theoret. Nanosci. **11**, 1–9 (2014).
32. N. Bachok, A. Ishak, and I. Pop, "Boundary Layer Stagnation-Point Flow and Heat Transfer over an Exponentially Stretching/Shrinking Sheet in a Nanofluid," Int. J. Heat Mass Transfer **55**, 8122–8128 (2012).
33. H. F. Oztop and E. Abu-Nada, "Numerical Study of Natural Convection in Partially Heated Rectangular Enclosures Filled with Nanofluids," Int. J. Heat Fluid Flow **29**, 1326–1336 (2008).
34. M. Q. Brewster, *Thermal Radiative Transfer Properties* (John Wiley and Sons, New York, 1972).